GPS Solutions (2022) 26:142
https://doi.org/10.1007/s10291-022-01326-z

ORIGINAL ARTICLE

UTC and GNSS system time access using PPP with broadcast ephemerides

Luca Carlin[1] · Oliver Montenbruck[1] · Johann Furthner[2] · André Hauschild[1]

Received: 23 March 2022 / Accepted: 22 August 2022 / Published online: 17 September 2022

Abstract

The application of precise point positioning with broadcast ephemerides (PPP-BCE) is discussed as an alternative to the established all-in-view technique for multi-GNSS time transfer. It combines the use of broadcast ephemerides with low-noise carrier-phase observations for accessing GNSS system time scales and Coordinated Universal Time (UTC) with improved precision, and can be employed on stationary as well as mobile receivers in offline or real-time analyses. Using calibrated timing receivers, the method is shown to provide estimates of the GNSS-to-GNSS time offsets (XYTOs) with an accuracy at the 2 ns level. In the absence of prior calibrations, 0.5 ns consistency across different stations is achieved for GPS, Galileo, and BeiDou-3 after adjustment of systematic biases in comparison with calibrated reference stations or broadcast XYTO values. Furthermore, access to GNSS-specific UTC realizations can be obtained through predictions of the UTC offset from GNSS system time as provided in the broadcast ephemerides of individual constellations. The overall quality of the PPP-BCE-derived receiver clock offsets from UTC is assessed using calibrated receivers at various timing laboratories along with BIPM-provided UTC-UTC(k) measurements. Over the 1.5 years covered in the study, an accuracy of 1.8 ns for GPS and 2.5 ns for Galileo is demonstrated. For BeiDou, a slightly worse accuracy of 3 ns is obtained for a single timing laboratory over 9 months.

Keywords GNSS · Time transfer · UTC · GPST · GST · BDT

Introduction

Next to positioning, timing is a key application of GNSS with ever-increasing relevance for today's society. Specific use cases include the synchronization of power lines, millisecond share trades, and telecommunication networks (Lisi 2015). As a complement to two-way satellite time and frequency transfer (TWSTFT) via geostationary satellites, the GNSS common-view (CV) and all-in-view (AV) techniques are widely used for clock comparison on regional and continental baselines (Lewandowski and Thomas 1991; Levine 2008; Defraigne 2017). They are traditionally based on the evaluation of time-averaged pseudorange-residuals relative to modeled values for a known receiver position. The residuals are commonly exchanged in the Common GNSS Generic Time Transfer Standard exchange format (CGGTTS; Defraigne and Petit 2015) and provide direct estimates of the receiver clock offset from GPS Time (GPST), or another GNSS system time (GNSST). By differencing the residuals (in CV mode) or the receiver-minus-GPST offsets (in AV mode), clocks at different locations may be compared and synchronized. Coordinated Universal Time (UTC; Panfilo and Arias 2019) can be accessed through GNSS-CV/-AV measurements of national timing laboratories, which provide individual, laboratory-specific UTC(k) realizations. An approximation of UTC can be obtained by applying UTC-minus-GNSS Time offsets as transmitted in the broadcast navigation messages to the receiver offsets from GNSS Time.

✉ Luca Carlin
luca.carlin@dlr.de

Oliver Montenbruck
oliver.montenbruck@dlr.de

Johann Furthner
johann.furthner@dlr.de

André Hauschild
andre.hauschild@dlr.de

[1] German Space Operations Center, Deutsches Zentrum für Luft- und Raumfahrt (DLR), 82234 Wessling, Germany

[2] Galileo Competence Center, Deutsches Zentrum für Luft- und Raumfahrt (DLR), 82234 Wessling, Germany

In its common implementation (Defraigne and Petit 2015), GNSS-CV and -AV time transfer are restricted to pseudorange data from stationary receivers, and their precision is governed by broadcast ephemeris errors, residual code multipath, and receiver noise contributions, as well as the use of a static troposphere model. For increased performance, precise point positioning (PPP; Malys and Jensen 1990; Zumberge et al. 1997; Kouba et al. 2017) techniques may be applied to time and frequency transfer. These techniques make joint use of pseudorange and carrier-phase measurements and provide the receiver clock offset at each observation epoch w.r.t. the implicit time scale of a precise GNSS orbit and clock product (Defraigne and Baire 2011). Typically, the respective clock product time scale represents neither a GNSS system time scale nor any UTC realization, but differencing of PPP-based receiver clock offsets between sites enables high-precision clock phase comparison and accurate frequency transfer. Best results are nowadays obtained using "Integer-PPP," i.e., PPP with ambiguity fixing (Delporte et al. 2008), which enables frequency transfer over multi-day arcs with up to 10^{-16} accuracy (Petit et al. 2015). PPP time transfer provides access to UTC(k) realizations when using GNSS observations of a UTC laboratory as a reference. However, it cannot offer direct access to GNSS system time scales for common users since GNSS observations of the respective GNSST reference stations are not publicly disclosed by GNSS system providers.

As an alternative to the aforementioned techniques, we assess the use of PPP with broadcast ephemerides (PPP-BCE; Gunning et al. 2019; Carlin et al. 2021) for clock synchronization and time scale monitoring. PPP-BCE inherits the basic concepts of carrier-phase processing from PPP, but makes use of broadcast ephemerides instead of post-processed precise orbit and clock products or real-time correction data. The increasing quality of broadcast ephemerides, particularly for Galileo (Montenbruck et al. 2018), enables positioning at the few-decimeter level with a PPP-BCE approach (Hadas et al. 2019). The present study explores applications of this approach for timing and demonstrates that GNSS system time scales and UTC can be accessed with few nanoseconds accuracy for properly calibrated receivers. Compared to the common GNSS-CV/AV implementation, the PPP-BCE approach offers a better precision through the use of carrier-phase observations and can provide instantaneous time offset estimates at each observation epoch (Bar-Sever et al. 2021). The use of broadcast ephemerides provides access to individual system time scales and enables monitoring of broadcast GNSS-to-GNSS time offsets (XYTO) that are not normally accessible for PPP-based time transfer. Furthermore, monitoring of broadcast UTC-GNSST (XXUT) offsets can be supported with GNSS receivers at UTC(k) laboratories.

To visualize and clarify the naming conventions of the different time scales at play and the relations among them, the scheme in Fig. 1 offers a representation of the time scales for dual-constellation processing of GPS and Galileo. The two constellations were chosen as an example to keep the figure clear for the reader, given that the paper focuses mainly on these systems. However, the scheme applies in the same manner to other GNSS as well. Basically, GNSS observations and broadcast ephemerides provide information on the difference between receiver time and individual GNSS time scales, while complementary information on the inter-constellation time offset is provided through the broadcast XYTO. Furthermore, each GNSS offers predictions of its own system time with respect to a system-specific UTC realization. These realizations can finally be related to UTC by using regular observations of the UTC-UTC(k) reported in Circular T of the Bureau International des Poids et Mesures (BIPM).

In the next section, we will delve into the methodology of the analyses, illustrating the details of the algorithm and listing the types and sources of the data used. Following this, another section will focus on a first analysis of the estimation of GNSS-to-GNSS time offsets. A second analysis, addressing the access to the UTC time scales, is presented afterward. At last, the summary and the conclusions are presented in a final section.

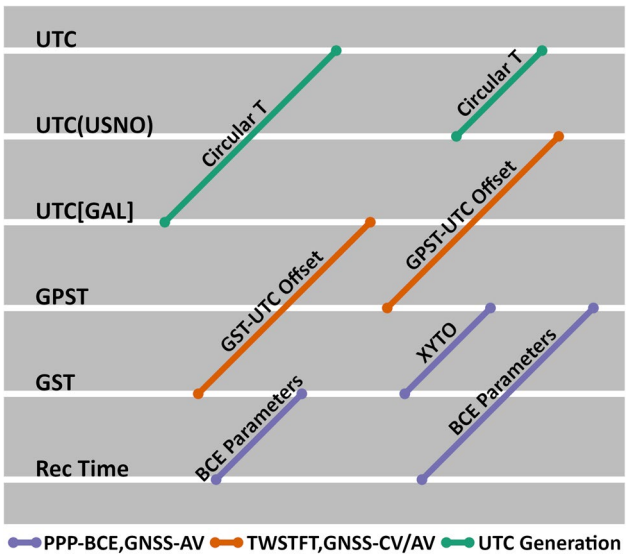

Fig. 1 Relations between the different time scales (white). The text on the diagonal lines indicates the parameter(s) used to translate from one time scale to the other, while the colors distinguish the employed methodology. For practical purposes, UTC[GAL] is approximated by the arithmetic average of UTC(IT), UTC(OP), UTC(PTB), UTC(ROA), and UTC(SP)

Data and methodology

The experiments conducted for this study build on the computation of the time and position of individual GNSS receivers covering different time intervals from March 2020 to October 2021. For this purpose, we used daily GNSS observations with 30 s sampling of 24 globally distributed multi-GNSS reference stations provided by the International GNSS Service (IGS; Johnston et al. 2017). In particular, five stations (BRUX, PTBB, ROAG, USN7/USN8) from selected time laboratories were included in order to take advantage of existing hardware calibrations and good stability of the receiver clocks, and the availability of UTC-UTC(k) monitoring results. The location of all sites is depicted in Fig. 2. All stations are equipped with geodetic-grade receivers providing pseudorange and carrier-phase measurements on at least two frequencies for the individual GNSS. The majority of the considered stations are equipped with Septentrio PolaRx5/5TR receivers supporting precise timing applications. In an effort to expand the analysis to at least one other type of receiver, a small amount of Javad TRE-G3TH and TRE_3 receivers were also included in the analysis. Both receiver types provide observations from semi-codeless P(Y) code tracking on the L1 and L2 frequency, which are designated as 1 W and 2 W in the Receiver Independent Exchange format (RINEX; Romero 2021) and compatible with the clock reference signals of the GPS broadcast ephemerides (SMSC 2021). For the Galileo FNAV (free navigation) ephemerides, satellite clock offsets are referred to pilot tracking of the E1 and E5a signals (EU 2021a). The corresponding 1Q and 5Q observations are made available by the PolaRx5TR receivers, while combined data + pilot-channel observations designated as 1X/5X are provided by the TRE-G3TH receivers. In the absence of suitable measurements of differential code bias (DCB) for pilot vs pilot + data tracking of the Galileo satellites, the respective biases have been ignored in the current analysis and are effectively lumped into the overall error budget for the affected stations. In the particular case of BeiDou-3, an ionospheric-free linear combination of pilot-only (1P/5P) or data + pilot-channel (1X/5X) observations of the modernized B1C and B2a signals is used in our processing. These signals employ the same frequency and similar modulations as the Galileo E1 and E5a signals and therefore promise reduced inter-system receiver biases compared to other signal options. Since all satellite clock offsets in BeiDou are referenced to the single-frequency B3I signal (CSNO 2017), the timing group delays obtained from the broadcast ephemerides need to be considered for the constellation. Due to the late deployment of receivers supporting B1C/B2a tracking of all satellites in the entire global BeiDou-3 constellation, we limit the BeiDou-3 analysis to a subset of two-thirds of all stations. No use of GLONASS is done in the present study due to frequency-channel-specific biases in FDMA signals that require channel-specific receiver calibrations for proper processing of pseudorange observations (GLONASS 2020) and hamper a consistent receiver time offset determination with common receivers.

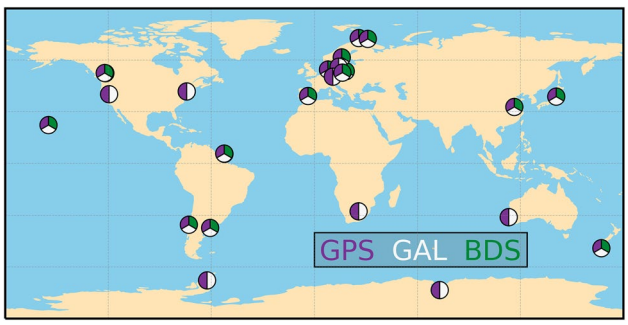

Fig. 2 Map of the receiver locations. The different symbols distinguish stations supporting Galileo (GAL) and BeiDou-3 (BDS) tracking in addition to GPS

The navigation messages required for the analyses, along with the GNSS-to-GNSS time offsets (XYTO) and UTC-to-GNSS time offset, were retrieved from the BRD400DLR RINEX navigation files provided by the IGS (Montenbruck and Steigenberger 2022). Among others, these files include merged broadcast ephemerides for GPS LNAV/CNAV, Galileo INAV/FNAV and BDS-3 CNAV-1/2/3 as well as system time offset (STO) polynomials for the individual constellations. The UTC-UTC(k) offsets for the selected timing laboratories, used to access the UTC time scale, were extracted from the Circular T files provided regularly by the BIPM (https://webtai.bipm.org/database/). The hardware calibrations for the selected stations of time laboratories were also retrieved from the BIPM website.

The PPP-BCE approach, introduced in Carlin et al. (2021) and used in this study, is based on a Kalman filter that estimates position, clock offset, wet tropospheric zenith delay, and ambiguities based on dual-frequency code and phase observations. In the present study, the elevation cut-off angle is set to 8°. The measurement model includes phase wind-up according to Wu et al. (1993) and an a priori troposphere model based on the Global Mapping Function (GMF) and the Global model of Pressure and Temperature (GPT) of Boehm et al. (2006, 2007). The ionospheric delay is removed up to the first order using dual-frequency ionosphere-free combinations. The carrier-phase ambiguities are treated as floating values instead of as fixed integers; they are also lumped together with the fractional phase biases and signal-in-space range errors into a single "pseudo-ambiguity" parameter for each tracked satellite (Wang et al., 2015). Process noise for the pseudo-ambiguities is chosen in accordance with the broadcast ephemeris quality and allows

at least partial compensation of the ephemeris errors (Carlin et al. 2021). In the observation model, the receiver time offset is formulated to refer to one constellation, plus an additional parameter per constellation considering the "User XYTO" (Defraigne et al. 2021). This value combines the receiver-specific inter-system biases (ISBs) with the XYTO system-time offset, and it is equal to zero by definition for the reference constellation. The User XYTO parameter is modeled as a random walk parameter, with a process noise standard deviation of 0.005 ns over a period of 30 s.

The basic observation model for pseudorange (p) and carrier-phase (φ) measurements is described by the relations

$$\begin{aligned} p &= \rho(\boldsymbol{r}_r) + c\left(\mathrm{d}t_{r,X} - \mathrm{d}t_Y^s + \Delta t_{XY}\right) + \left(T + m\mathrm{d}T_z\right) + B_{r,Y} + B_Y^s \\ \varphi &= \rho(\boldsymbol{r}_r) + c\left(\mathrm{d}t_{r,X} - \mathrm{d}t_Y^s + \Delta t_{XY}\right) + \left(T + m\mathrm{d}T_z\right) + A^s + \Psi^k \end{aligned} \tag{1}$$

here it is assumed that ionospheric path delays are eliminated to first order in the "ionospheric-free" linear combination of dual-frequency observations and can therefore be neglected in the observation model. Within the above equations, ρ denotes the light-time corrected, geometric distance between the receiver at position $\boldsymbol{r}_r$ and the observed satellite of constellation Y, c is the speed of light in vacuum, and $\mathrm{d}t_{r,X}$ is the receiver clock offset with respect to the system time of a constellation X, which is selected as the reference for the receiver time determination. $\mathrm{d}t_Y^s$ is the satellite clock offset with respect to the system time of the observed constellation Y, and $\Delta t_{XY} = t_Y - t_X$ is the XYTO system time offset of constellation Y with respect to X. The latter term vanishes when processing observations of the reference constellation, i.e., for $Y = X$. The modeled troposphere delay is described by T, while m and $\mathrm{d}T_z$ denote the elevation-dependent mapping function and a zenith delay correction to the a priori model, respectively. Finally, A^s is the carrier-phase pseudo-ambiguity, $B_{r,Y}$ and B_Y^s denote the receiver and satellite code biases for the ionosphere-free combination of dual-frequency observations relative to the clock reference signals (or signal) of constellation Y, and Ψ is the carrier-phase wind-up.

For calibrated receivers, the receiver biases can be applied directly in the observation model. Satellite biases vanish if the observed signals match the reference signals defined for the clock offsets of the corresponding constellation. This is readily possible for GPS and Galileo by selecting 1 W/2 W and 1Q/5Q observations, respectively. For BeiDou-3, in contrast, the use of satellite code biases is inevitable since broadcast clocks are referenced to the single-frequency B3I signal. The required values are provided in the form of timing group delay (TGD) parameters as part of the CNAV-1/2 navigation messages for the B1C and B2a signal.

Subject to the availability of all bias parameters, the unknowns $\boldsymbol{r}_r$, $\mathrm{d}t_{r,X}$, Δt_{XY}, and $\mathrm{d}T_z$ as well as the vector of pseudo-ambiguities $\boldsymbol{A}^s$ for all tracked satellites can then be estimated in the Kalman filter, while the remaining parameters of the observation model constitute modeled values. For uncalibrated receivers, unknown receiver biases will effectively be lumped into the other estimation parameters without changing the basic structure of the observation model:

$$\begin{aligned} p &= \rho + c\left(\overline{dt}_{r,X} - dt_Y^k + \overline{\Delta t}_{XY}\right) + \left(T + mdT_z\right) + B_Y^s \\ \varphi &= \rho + c\left(\overline{dt}_{r,X} - dt_Y^k + \overline{\Delta t}_{XY}\right) + \left(T + mdT_z\right) + \overline{A}^s + \Psi^k \end{aligned} \tag{2}$$

here bars are used to designate the lumped quantities

$$\begin{aligned} c\overline{\mathrm{d}t}_{r,X} &= c\mathrm{d}t_{r,X} + B_{r,X} \\ c\overline{\Delta t}_{\mathrm{XYTO}} &= c\Delta t_{XY} + \left(B_{r,Y} - B_{r,X}\right) \\ \overline{A}^s &= A^s - B_{r,Y} \end{aligned} \tag{3}$$

i.e., the biased receiver clock offset, the User XYTO, and a modified pseudo-ambiguity.

In the given formulation, the algorithm directly provides the receiver clock offset $\mathrm{d}t_{r,X}$ or a biased value $\overline{\mathrm{d}t}_{r,X}$ thereof relative to the system time scale of the selected reference constellation. If needed, receiver clock offsets for other tracked constellations can then be obtained by adding the corresponding estimate of the XYTO or User XYTO. Receiver clock offsets from UTC can furthermore be obtained by adding constellation-specific UTC offsets transmitted in the broadcast ephemerides.

Even though the PPP-BCE method is only applied in offline analyses and for stationary receivers, we emphasize that the method is not restricted to these conditions. Since the receiver antenna position is treated as an independent estimation parameter of the Kalman filter, the method is likewise applicable for time synchronization of moving receivers. Depending on the speed of motion, process noise in the position state can be used to compensate for position changes between epochs or an additional velocity state can be included as discussed in Carlin et al (2021). Furthermore, real-time operation is enabled by the purely sequential processing of observations in the Kalman filter.

GNSS-to-GNSS time offsets

Monitoring of inter-system time offsets constitutes a first application of the PPP-BCE method and is discussed in this section. Starting with GPS and Galileo, User GPS-to-Galileo Time Offsets (GGTO) values were computed for the 28 stations in individual Kalman-filter runs covering a 30-days period starting on day-of year (DOY) 181, 2021. The results are depicted in Fig. 3 and show that the methodology can

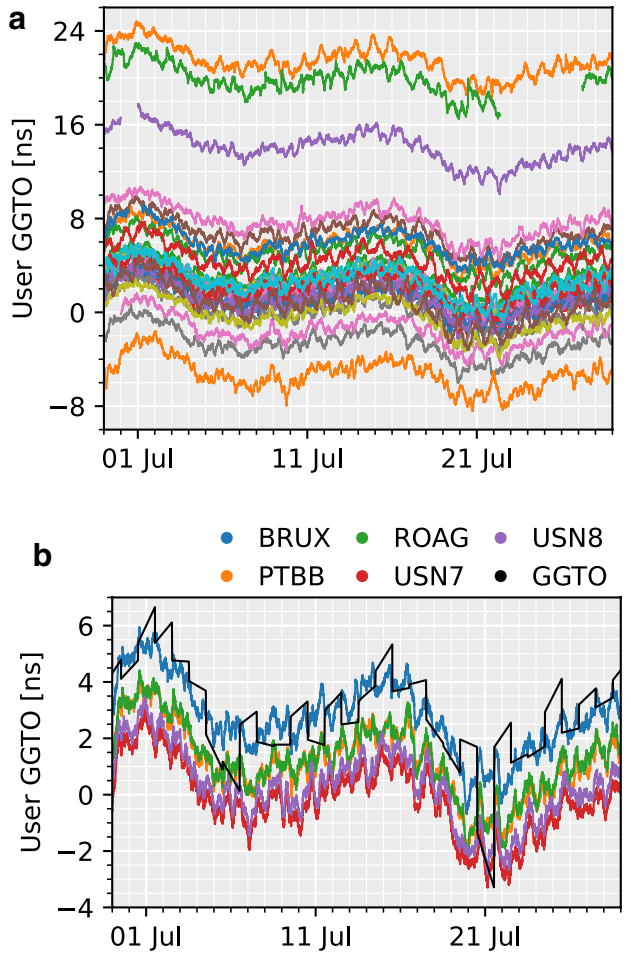

Fig. 3 Estimated User GGTO for all stations (top) and GGTO estimate of calibrated timing receivers (bottom) in the period DOY 181–210, 2021. Individual stations are distinguished by different colors. For reference, the bottom plot also shows the values of the broadcast GGTO value transmitted by the Galileo satellites

provide a smooth and continuous estimate of the User GGTO at the individual observation epochs for all stations. The User GGTO estimates of individual stations show a common overall variation with peak to peak amplitude of about 5 ns over the analysis period but differ by site-specific offsets and sub-daily variations.

The offset corresponds to the ISB introduced by the receiver hardware and can be corrected for the receivers at international timing laboratories using the GPS/Galileo hardware delays obtained in calibrations with a traveling reference receiver (BIPM 2020). For these receivers, the mean offset with respect to the broadcast GGTO ranges from zero to 3 ns for the individual stations, which is slightly larger than expected from the 1.5 ns uncertainty of the BIPM calibrations. For other stations, a cross-calibration with respect to the calibrated ones can be performed. Figure 4 provides the same results of Fig. 3 after removing the mean User

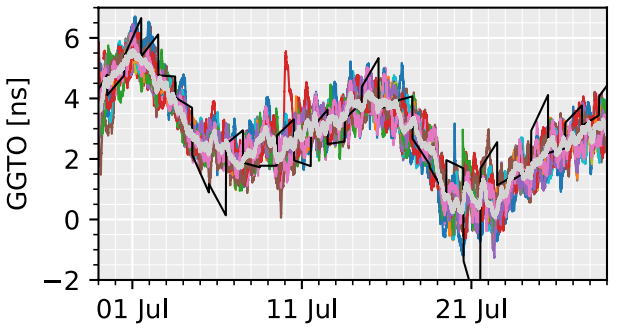

Fig. 4 Estimated GGTO for DOY 180–210, 2021 after adjustment and removal of site-specific User GGTO biases relative to the BRUX station. Individual stations are distinguished by different colors. The epoch-wise mean over all stations is indicated by a bold gray line. Furthermore, the broadcast GGTO is superimposed as a black line for reference

GGTO difference with respect to BRUX. Following the alignment, GGTO estimates from individual stations show consistency of 0.3–0.6 ns (1σ) with the epoch-wise mean GGTO of all stations. This evidences a favorable precision of the PPP-BCE method and shows that the accuracy of GGTO estimates is mainly driven by the quality of receiver hardware calibrations.

Figure 4 illustrates that all stations can consistently estimate the GGTO independently of the location and receiver type. After removal of site-specific biases, the difference between the stations lies primarily in the sub-daily variations, which show oscillations in the order of 1 ns amplitude. These reflect the quality of the broadcast orbit and clock predictions for the set of tracked satellites and therefore depend on the location and time of day.

In order to further confirm the capability of the PPP-BCE method to estimate the GGTO, a long-term analysis was performed for station BRUX, computing quasi-monthly (30-days) batch solutions from March 2020 until October 2021. The results, depicted in Fig. 5, illustrate once again a good agreement between the estimated and broadcast GGTO, with a root mean square (RMS) consistency of 1.8 ns, which is well within the 20 ns (95th percentile) requirement for the difference between the broadcast and true GGTO established for the Galileo Initial Services (EU 2021b). Except for August 2021, when the GGTO reached values above 18 ns, the difference between GPST and Galileo System Time (GST) is mostly bounded within $\pm$ 10 ns.

More information about the sub-daily variations of the GGTO, as well as the big deviation of August 2021, can be found by looking at the receiver clock offsets. In particular, using a highly stable receiver clock, such as the ones from time laboratories, can be useful to characterize the actual system times. The receiver clock offsets of the BRUX station

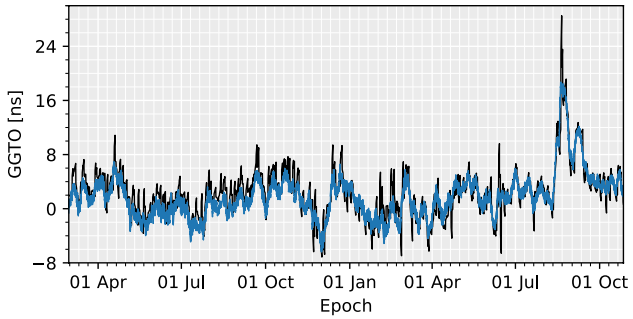

Fig. 5 Comparison of GGTO obtained in the PPP-BCE analysis for the calibrated BRUX station (blue) with broadcast GGTO values from the Galileo navigation message (black). The period is Feb 29, 2020, to Oct 27, 2021

from GPST and GST obtained with consideration of the site-specific hardware biases (BIPM 2020) are depicted as an example in Fig. 6. Immediately, it can be noticed that the pronounced increase in the GGTO value of August 2021 is caused by a deviation of GST from the highly stable BRUX time scale. The same variation of GST is present in the receiver clock offsets of PTBB, ROAG and USN8 for the same period and is confirmed by the UTC-UTC_{GAL} values retrieved from the navigation message. Again, however, the observed GST variation is well within the overall limit of < 30 ns (95th percentile) UTC dissemination error established in the Galileo Initial Services specification (EU 2021b). Apart from this specific case, the sub-daily variations of the User GGTO seem to be driven by the broadcast realization of GPST. The overall performance of broadcast GPST is limited by the accuracy of the broadcast ephemeris, as well as a possible impact of flex power that has been intensively used in recent years (Esenbuga and Hauschild 2020; Xiang et al. 2020). The broadcast realization of GST appears to be more stable, confirming that the better quality of the Galileo broadcast ephemerides (Montenbruck et al. 2018) benefits the system time access as well.

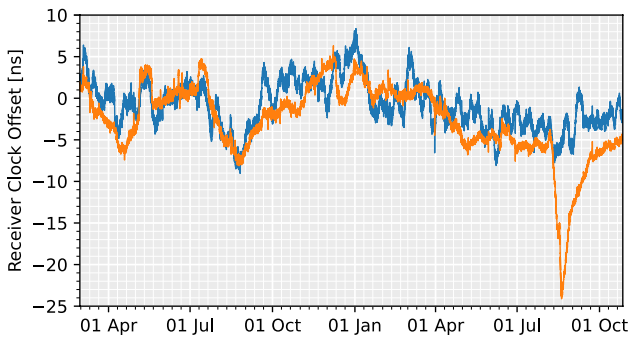

Fig. 6 BRUX receiver time offset from GPST (blue) and GST (orange) based on PPP with GPS and Galileo observations and broadcast ephemerides between March 2020 and October 2021

Complementary to the GGTO, we analyzed the offset of Galileo System Time (GST) from BeiDou System Time (BDT), i.e., the BGTO, based on B1C/B2a and E1/E5a observations from a total of 19 contributing stations equipped with either PolaRx (17) and TRE (2) receivers. Other than for GPS and Galileo, dedicated receiver hardware calibrations are not presently available for BeiDou-3 tracking, but the commonality of frequencies and modulation schemes (Betz 2016) of the signals used in our analysis suggests that at least analog biases in the reception chain should cancel in the User BGTO estimation. Due to the fact that BeiDou system time refers to the B3I signal, satellite group delays between B3I and the ionosphere-free B1C/B2a combination must be considered in the analysis. The required timing group delays (TGDs) are taken from the CNAV-1 and CNAV-2 broadcast navigation messages. Other than current IGS code bias products, the broadcast TGD values are accessible in real-time and are not aligned to zero constellation mean but rather the hardware calibration of a single reference satellite (Wu et al. 2011; Montenbruck et al 2022). Despite potential incompatibilities between common user equipment and the TGD determination in the BeiDou control segment (Zhang et al. 2020; Montenbruck et al. 2022), the broadcast group delays are, therefore, preferred over the potentially more precise IGS products for timing analyses.

Figure 7 depicts the User BDGA of all considered stations, their mean value, and the broadcast BGTO made available in the CNAV-1/2 navigation messages of BeiDou-3.

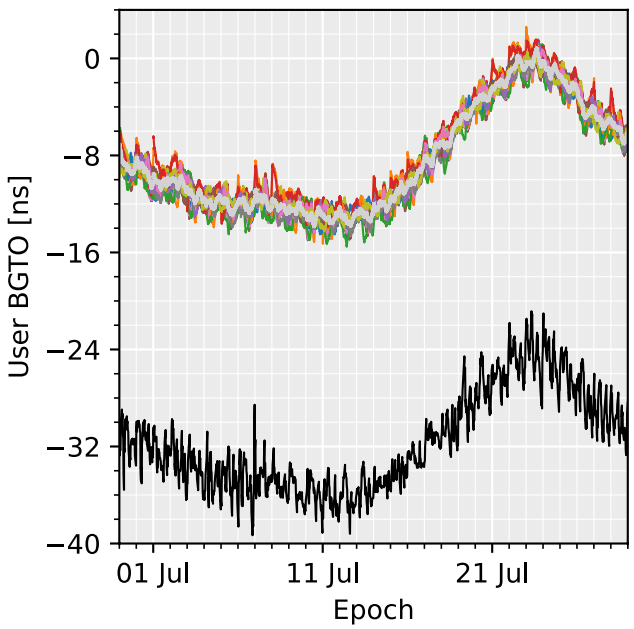

Fig. 7 Estimated BeiDou-to-Galileo system time offsets and broadcast BGTO (black) for DOY 181–210, 2021. Next, the values for User BGTO for individual stations are distinguished by individual colors; a bold gray line indicates their mean value

Despite the use of different receivers, cables, and antennas, the results of individual stations show a remarkable consistency, which confirms the previously assumed compatibility of Galileo E1/E5a hardware delays with those of BeiDou B1C/B2a. Overall, individual BGTO estimates exhibit a 0.5 ns RMS error relative to the mean of all stations, which reflects an almost 3 times lower point-to-point scatter than the broadcast BGTO. In addition, a systematic 24 ns difference between the User BGTOs and the broadcast BGTO can be observed. While the cause of this offset cannot be identified with certainty, it may be noted that a much better consistency at the 5 ns level is obtained when comparing the User BGTOs with a BGTO reconstructed from the UTC-GST and UTC-BDT offsets transmitted in the Galileo and BeiDou navigation messages. As such, a systematic bias in the GST estimation at the BeiDou control center is supposed. However, improvements may be expected from the recent installation calibration of a new multi-GNSS timing receiver at the BeiDou control center (Li et al. 2021). Meanwhile, the PPP-BCE method presented in the current study offers a suitable alternative for BGTO estimation in common geodetic receivers.

UTC time offsets

Access to UTC for GNSS users is provided through polynomial predictions of the offset between the system-specific UTC reference and the respective GNSS system time scale transmitted as part of the navigation messages. The accuracy of these predictions is strongly influenced by the system and the navigation message type. GPS LNAV, Galileo INAV/FNAV, and BDS D1/D2 messages all have limited resolution, in the order of 1 ns, and only offer a 1st-degree polynomial prediction, while newer messages such as GPS CNAV/CNAV-2 and BDS-3 CNAV-1/2/3 provide improved granularity and a 2nd order polynomial.

Furthermore, allowance must be made for each GNSS system time is controlled and monitored with respect to a different GNSS-specific UTC realization (UTC_{GNSS}). For GPS, this reference is UTC(USNO), while for BeiDou it corresponds to UTC(NTSC). Galileo is a special case in this context; instead of using a single UTC(k) realization, it is monitored against a blend of five timing laboratories, including UTC(IT), UTC(PTB), UTC(OP), UTC(ROA), and UTC(SP) (Piriz et al. 2015). The notation for the Galileo UTC reference is henceforward set to UTC[GAL], with the square brackets highlighting its relation to the UTC realization of more than a single laboratory. The details of how this blend is obtained are not publicly disclosed; therefore, we assume UTC[GAL] to be equal to the arithmetic mean of the five UTC(k) values. The offsets between the mentioned

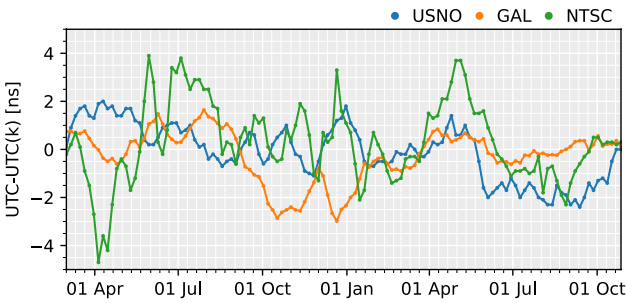

Fig. 8 Offsets between UTC and GNSS-specific UTC realizations, as extracted from BPIM Circular T. RMS values for UTC realizations referenced by GNSS providers range from 1.1 ns for UTC(USNO) and UTC[GAL] to 1.7 ns for UTC(NTSC)

time references and UTC are typically at the few ns level and are shown in Fig. 8 for the period concerning our analysis.

For converting the receiver time offset from GNSS system time to receiver offsets from UTC_{GNSS}, we made use of the highest-resolution UTC offset information in the BRD400DLR RINEX navigation files. Once the receiver clock offsets refer to the GNSS-specific UTC reference, e.g., UTC(USNO) and UTC[GAL], they can be related to UTC by removing the UTC-UTC_{GNSS} difference shown in Fig. 8 and extracted from the BIPM Circular T products. As a result, independent estimates of the receiver clock offsets from UTC are obtained for each of the considered GNSS.

Since the time of calibrated receivers used in time laboratories effectively represents UTC(k), plus a known offset from UTC that is provided in the BIPM Circular T, these receivers can be used as a reference against which the UTC offsets obtained through the PPP-BCE chain can be compared. The differences for the receivers BRUX, PTBB, ROAG and USN8 as obtained through GPS and Galileo observations over a 1.5-year interval are depicted in Fig. 9, color-coded for each constellation. Across all stations, the RMS error of UTC access is 1.8 ns and 2.5 ns, for GPS and Galileo, respectively.

The values of Fig. 9 show a strong agreement among four stations irrespective of their location. Unexpectedly, while better broadcast ephemerides characterize Galileo with respect to GPS, it shows a slightly inferior performance when it comes to accessing UTC. This suggests that the determination of receiver time offsets from UTC is ultimately dominated by errors in the predicted offsets of GNSS time and UTC_{GNSS} transmitted by the system providers rather than the PPP-BCE-based access to the GNSS system time itself.

Errors of the estimated receiver time offset estimates from UTC as obtained with BeiDou-3 are shown in Fig. 10, which also provides the corresponding Galileo-based results for comparison. Similar to the BGTO estimation, lacking hardware calibrations for BDS B1C and B2a signals have

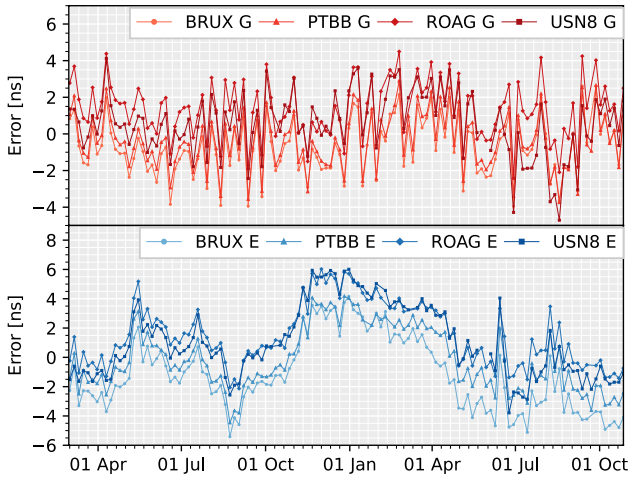

Fig. 9 Total error of UTC access through PPP-BCE chain based on GPS (G; top) and Galileo (E; bottom) observations with calibrated receivers at selected timing laboratories between March 2020 and October 2021

been substituted by the Galileo E1 and E5a delays. Given the limited support of BeiDou-3 observations, only two timing laboratories and a reduced overall data period are considered here. For the BRUX station, UTC errors from both constellations are of similar magnitude (approx. 3 ns RMS) in the 9 months interval, even though the difference between BeiDou- and Galileo-based UTC estimates attains peak values of up to 10 ns in the second half of the year. Results for ROAG exhibit a 4 ns bias with respect to BRUX, which can also be identified in the Galileo-based UTC results of Fig. 9. This bias reflects an inferior consistency of hardware delay calibrations for E1/E5a signals across the two stations as compared to corresponding GPS L1/L2 results and directly impacts the overall accuracy of UTC access with multi-GNSS observations.

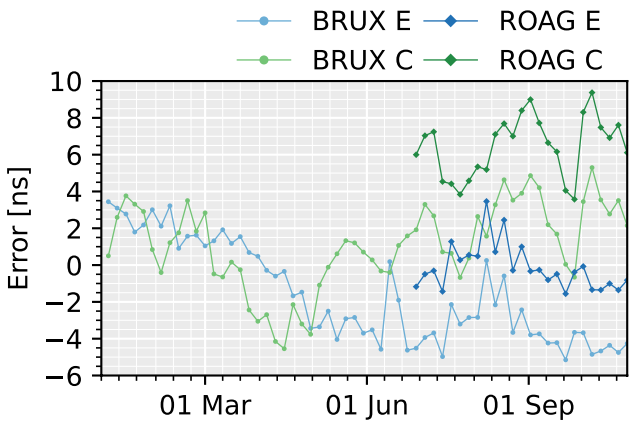

Fig. 10 Total error of UTC access through PPP-BCE chain based on BeiDou-3 (C) and Galileo (E) observations with calibrated receivers at two timing laboratories between January 2021 and October 2021

Summary and conclusions

Established techniques for GNSS-based time and frequency transfer may largely be divided into code-based methods using broadcast ephemerides and precise point positioning with precise GNSS ephemerides. While the former can provide direct access to GNSS system scales and, optionally, UTC for standalone receivers but suffers from limited precision and accuracy, the latter supports high-precision time transfer and highly accurate frequency transfer between two sites. Within this study, the combination of carrier-phase-based precise point positioning and broadcast ephemerides (PPP-BCE) is assessed as a tool for GNSS system time monitoring as well as access to international time scales. Compared to code-based processing, the PPP approach offers enhanced precision, while the use of broadcast ephemerides rather than precise products enables a direct link between receiver time and GNSS system time scales. Using the predictions included in the broadcast ephemerides, the UTC reference of the GNSS system times can be accessed, which can in turn be related to UTC through UTC-UTC(k) offsets reported in the BIPM Circular T products. When working with a sequential estimation technique, such as the Kalman filter adopted in the present study, the PPP-BCE method can support precise timing in real-time applications and is equally applicable for stationary and mobile platforms.

The use of carrier-phase observations allows for smoother time offset estimates than purely pseudorange-based methods and the achievable precision of receiver-time offsets from GNSS time is largely driven by the quality of the broadcast ephemerides. Access to GPS system time is slightly worse than for Galileo system time due to a worse broadcast ephemeris accuracy and possibly sub-daily code bias variations related to the current use of flex power transmission. Overall, these effects cause variations at 1 ns level in the estimated receiver time offset from GPST. A similar precision is achieved for BeiDou, while Galileo offers a roughly two times better performance. Inter-constellation system-time offsets between GPS, Galileo, and BeiDOu-3 can be monitored from individual stations with a representative precision of 0.5 ns (1σ). This performance is generally better than that of broadcast XYTO values and can further be improved by averaging over multiple globally distributed stations. Thus, the PPP-BCE method is a practical tool for inter-system time offset determination that can readily be integrated into real-time integrity monitoring systems for multi-GNSS users.

In terms of accuracy, both the access to GNSS time scales and the determination of system time differences depend on proper hardware calibrations of the employed receivers. Comparing GGTO results from

various international timing results, inconsistencies of about ± 2 ns could be identified that reflect the present accuracy in the determination of analog and digital delay differences between tracking of L1/L2 GPS signals and E1/E5a Galileo signals. For the BeiDou-to-Galileo time offset, a notably better consistency (< 0.1 ns mean difference) of User BGTOs was observed even for uncalibrated receivers, which reflects a high commonality of the respective hardware biases for the interoperable B1C/B2a and E1/E5a signals in currently available geodetic receivers. On the other hand, access to BeiDou system time using dual-frequency GNSS observations depends on the knowledge of differential code biases for the BeiDou-3 satellites. So far, only broadcast group delays relate to an absolute calibration but are generally considered to be less precise than dedicated DCB products of the International GNSS Service.

Access to UTC using the PPP-BCE approach has been demonstrated with calibrated GNSS receivers at selected timing laboratories. Here, RMS errors of 1.8 ns and 2.5 ns have been obtained for GPS and Galileo, respectively, when taking into account the UTC-UTC(k) offsets as reported by the BIPM. These offsets exhibit RMS values of typically 1–2 ns for the various UTC laboratories referenced in broadcast UTC-GNSST predictions of individual GNSS providers. Without their consideration, the accuracy of estimated receiver offsets from UTC would degrade to roughly 2–3 ns when working with GPS and Galileo. For BeiDou, absolute hardware calibrations are not presently available, and BDT, as well as UTC access, relies essentially on relative calibrations in relation to other GNSS constellations. For a well-calibrated station, a 3 ns accuracy could be achieved in the determination of receiver time offsets from UTC using BeiDou-3 observations along with the respective broadcast ephemerides, differential code biases, and BDT-UTC offset predictions over 9 months. However, systematic biases of up to 4 ns were likewise evident among different timing stations that reflect remaining calibration uncertainties for the constellations and signals.

Acknowledgements We gratefully acknowledge public provision of GNSS data and auxiliary products used in this study through the International GNSS Service, as well as the Bureau International des Poids et Mesures (BIPM).

Funding Open Access funding enabled and organized by Projekt DEAL.

Data availability This study makes use of RINEX observation data and broadcast navigation data publicly available from the data archives of the International GNSS Service (IGS) at https://cddis.nasa.gov/archive and ftp://igs-rf.ign.fr/. Calibration data for the timing station are provided freely by the Bureau International des Poids et Mesures (BIPM) at https://webtai.bipm.org/ftp/pub/tai/.

References

Bar-Sever Y, Meyer R, Muthuraman K, Biacs Z (2021) Monitoring and performance assessment of GNSS inter-constellation timescale biases. In: Proceedings of ION GNSS+ 2021, Institute of Navigation, St. Louis, Missouri, September 20–24, 1903–1916. https://doi.org/10.33012/2021.17983

Betz J (2016) Engineering satellite-based navigation and timing—global navigation satellite systems, signals, and receivers. Wiley-IEEE Press

BIPM (2020) 2018 Group 1 GNSS calibration trip (Cal_Id 1001-2018) Summary, v2.0, 20 June 2020; URL https://webtai.bipm.org/ftp/pub/tai/publication/time-calibration/Current/1001-2018_GPSP3C1-GALE3_Group1-trip_V2-0.pdf

Boehm J, Niell AE, Tregoning P, Schuh H (2006) Global Mapping Function (GMF): a new empirical mapping function based on numerical weather model data. Geophys Res Lett 33:L07304. https://doi.org/10.1029/2005GL025545

Boehm J, Heinkelmann R, Schuh H (2007) Short note: a global model of pressure and temperature for geodetic applications. J Geod 81(10):679–683. https://doi.org/10.1007/s00190-007-0135-3

Carlin L, Hauschild A, Montenbruck O (2021) Precise point positioning with GPS and Galileo broadcast ephemerides. GPS Solut 25(2):77. https://doi.org/10.1007/s10291-021-01111-4

CSNO (2017) BeiDou navigation satellite system signal in space interface control document open service signal B1C. China Satellite Navigation Office, Dec. 2017

Defraigne P (2017) GNSS time and frequency transfer. In: Teunissen P, Montenbruck O (eds) Springer handbook of global navigation satellite Systems. Springer, Cham, pp 1187–1206. https://doi.org/10.1007/978-3-319-42928-1_41

Defraigne P, Baire Q (2011) Combining GPS and GLONASS for time and frequency transfer. Adv Space Res 47(2):265–275. https://doi.org/10.1016/j.asr.2010.07.003

Defraigne P, Petit G (2015) CGGTTS-version 2E: an extended standard for GNSS time transfer. Metrologia 52(6):G1. https://doi.org/10.1088/0026-1394/52/6/G1

Defraigne P, Pinat E, Bertrand B (2021) Impact of Galileo-to-GPS-time-offset accuracy on multi-GNSS positioning and timing. GPS Solut 25(2):45. https://doi.org/10.1007/s10291-021-01090-6

Delporte J, Mercier F, Laurichesse D, Galy O (2008) GPS carrier-phase time transfer using single-difference integer ambiguity resolution. Int J Navig Obs 2008:273785

Esenbuğa ÖG, Hauschild A (2020) Impact of flex power on GPS Block IIF differential code biases. GPS Solut 24(4):91. https://doi.org/10.1007/s10291-020-00996-x

EU (2021a) European GNSS (Galileo) Open Service Signal-In-Space Interface Control Document (OS SIS ICD) issue 2.0, European Union

EU (2021b) European GNSS (Galileo) Open Service Service Definition Document (OS SDD) Issue 1.2, European Union

GLONASS (2020) Global navigation satellite system GLONASS Open Service Performance Standard (OS PS) Appendix B background information, ed. 2.2, Korolev

Gunning K, Blanch J, Walter T (2019) SBAS corrections for PPP integrity with solution separation. In: Proceedings of ION ITM 2019, Reston, VA, USA, January 28–31, pp 707–719. https://doi.org/10.33012/2019.16739

Hadas T, Kazmierski K, Sośnica K (2019) Performance of Galileo-only dual-frequency absolute positioning using the fully serviceable Galileo constellation. GPS Solut 23(4):1–2. https://doi.org/10.1007/s10291-019-0900-9

Johnston G, Riddell A, Hausler G (2017) The international GNSS service. In: Teunissen PJG, Montenbruck O (eds) Springer handbook of global navigation satellite systems, chap. 33. Springer International Publishing, Cham, pp 967–982. https://doi.org/10.1007/978-3-319-42928-1_33

Kouba J, Lahaye F, Tétreault P (2017) Precise point positioning. In: Teunissen PJG, Montenbruck O (eds) Springer handbook of global navigation satellite systems, chap. 25. Springer International Publishing, Cham, pp 723–752. https://doi.org/10.1007/978-3-319-42928-1_25

Levine J (2008) A review of time and frequency transfer methods. Metrologia 45:S162–S174. https://doi.org/10.1088/0026-1394/45/6/S22

Lewandowski W, Thomas C (1991) GPS time transfer. Proc IEEE 79(7):991–1000. https://doi.org/10.1109/5.84976

Li G, Zhang D, Lin Y, Wang JA (2021) Closed-loop calibration method of the BeiDou time receiver. In: Yang C, Xie J (eds) China satellite navigation conference (CSNC 2021) proceedings, LNEE 774, pp 74–85. https://doi.org/10.1007/978-981-16-3146-7_8

Lisi M (2015) GNSS or GTSS? The increasing and strategic role of global navigation satellite systems as precise timing reference for critical infrastructures. In: 21st Ka and broadband communications conference—satellites and the internet, October 12–14, Bologna

Malys S, Jensen PA (1990) Geodetic point positioning with GPS carrier beat phase data from the CASA UNO experiment. Geophys Res Lett 17(5):651–654. https://doi.org/10.1029/GL017i005p00651

Montenbruck O, Steigenberger P (2022) BRD400DLR: DLR's merged multi-GNSS broadcast ephemeris product in RINEX 4.00 format DLR/GSOC. https://doi.org/10.57677/BRD400DLR

Montenbruck O, Steigenberger P, Hauschild A (2018) Multi-GNSS signal-in-space range error assessment—methodology and results. Adv Space Res 61(12):3020–3038. https://doi.org/10.1016/j.asr.2018.03.041

Montenbruck O, Steigenberger P, Wang N, Hauschild A (2022) Characterization and performance assessment of BeiDou-2/3 satellite group delays. Navig J ION 69(3):navi.526. https://doi.org/10.33012/navi.526

Panfilo G, Arias F (2019) The coordinated universal time (UTC). Metrologia 56(4):042001. https://doi.org/10.1088/1681-7575/ab1e68

Petit G, Kanj A, Loyer S, Delporte J, Mercier F, Perosanz F (2015) 1 $\times 10^{-16}$ frequency transfer by GPS PPP with integer ambiguity resolution. Metrologia 52(2):301. https://doi.org/10.1088/0026-1394/52/2/301

Piriz R, Rodríguez D, Roldán P, Mudrak A, Bauch A, Riedel F, Staliuniene E, Galindo J, Esteban H, Sesia I, Cerretto G (2015) The time validation facility (TVF): an all-new key element of the Galileo operational phase. In: IEEE international frequency control symposium & the European frequency and time forum 2015 April 12, pp 320–325. https://doi.org/10.1109/FCS.2015.7138851

Romero I (ed) (2021) RINEX the receiver independent exchange format version 4.00, 1 Dec 2021

SMSC (2021) NAVSTAR GPS space segment/navigation user interfaces. IS-GPS-200, Rev. M, Space and Missile Systems Center, Los Angeles Airforce Base, May 21, 2021

Wang F, Gong X, Sang J, Zhang X (2015) A novel method for precise onboard real-time orbit determination with a standalone GPS receiver. Sensors 15(12):30403–30418. https://doi.org/10.3390/s151229805

Wu JT, Wu SC, Hajj G, Bertiger WI, Lichten SM (1993) Effects of antenna orientation on GPS carrier phase. Manuscr Geodaet 18(2):91–98

Wu X, Ping J, Liu L, Xing N (2011) Hardware delay solution of regional satellite navigation system. Geomat Inf Sci Wuhan Univ 36(10):1218–1221 (**in Chinese**)

Xiang Y, Xu Z, Gao Y, Yu W (2020) Understanding long-term variations in GPS differential code biases. GPS Solut 24(4):118. https://doi.org/10.1007/s10291-020-01034-6

Zhang Y, Kubo N, Chen J, Chu FY, Wang A, Wang J (2020) Apparent clock and TGD biases between BDS-2 and BDS-3. GPS Solut 24(1):27. https://doi.org/10.1007/s10291-019-0933-0

Zumberge JF, Heflin MB, Jefferson DB, Watkins MB, Webb FH (1997) Precise point positioning for the efficient and robust analysis of GPS data from large networks. J Geophys Res 102(B3):5005–5017. https://doi.org/10.1029/96JB03860

Luca Carlin is a scientific staff member of the GNSS Technology and Navigation Group at DLR's German Space Operations Center (GSOC). His current work is centered on the development of Precise Point Positioning (PPP) techniques for multi-GNSS processing. He holds a bachelor's degree in Aerospace Engineering from Politecnico di Torino (Italy) and a master's degree in Earth Oriented Space Science and Technology from the Technical University of Munich (Germany).

Oliver Montenbruck is head of the GNSS Technology and Navigation Group at DLR's German Space Operations Center (GSOC). His research activities include spaceborne GNSS receiver technology, autonomous navigation systems, spacecraft formation flying and precise orbit determination, new constellations, and multi-GNSS processing. Dr. Montenbruck presently chairs the Multi-GNSS Working Group of the International GNSS Service and coordinates the performance of the MGEX Multi-GNSS Experiment. He is a fellow of the Institute of Navigation (ION) and received the ION Johannes Kepler Award in 2018.

Johann Furthner is head of the Signal Analysis and Timing Systems department at DLR's Galileo Competence Center, where he works on general GNSS performance analysis, signal verification, calibration processes and timing aspects. He received his Ph.D. in Laser Physics from the University of Regensburg in 1994, Germany, and has been working in the field of navigation at DLR's Institute of Communications and Navigation at the German Aerospace Center (DLR) from 1995 to 2019. In 2008/2009, he served as a Navigation Performance Engineer in the Galileo Project Team at ESA/ESTEC.

André Hauschild is a researcher in the GNSS Technology and Navigation Group at DLR/GSOC in Oberpfaffenhofen. His field of work focuses on real-time precise clock estimation for GNSS satellites as well as multi-GNSS processing using modernized GPS and new satellite navigation constellations. He is involved in projects with spaceborne GNSS receivers for precise orbit determination of satellites, radio occultation and launcher trajectory determination. Dr. Hauschild graduated in aerospace engineering from Technical University Brunswick (TU BS), Germany, in March 2007 and received his doctoral degree from Technical University Munich (TUM), Germany, in July 2010. He was awarded the ION Tycho Brahe Award in 2020.